

# DNA damage response as a candidate anti-cancer barrier in early human tumorigenesis

Jirina Bartkova<sup>1</sup>, Zuzana Hořejší<sup>1,5</sup>, Karen Koed<sup>2</sup>, Alwin Krämer<sup>1</sup>, Frederic Tort<sup>1</sup>, Karsten Zieger<sup>2</sup>, Per Guldborg<sup>1</sup>, Maxwell Sehested<sup>3</sup>, Jahn M. Nesland<sup>4</sup>, Claudia Lukas<sup>1</sup>, Torben Ørntoft<sup>2</sup>, Jiri Lukas<sup>1</sup> & Jiri Bartek<sup>1</sup>

<sup>1</sup>Institute of Cancer Biology and Centre for Genotoxic Stress Research, Danish Cancer Society, Strandboulevarden 49, DK-2100 Copenhagen, Denmark

<sup>2</sup>Department of Clinical Biochemistry, Aarhus University Hospital, Skejby, DK-8200 Aarhus N, Denmark

<sup>3</sup>Department of Pathology, University Hospital, Frederik V's Vej 11, DK-2100 Copenhagen, Denmark

<sup>4</sup>Department of Pathology, The Norwegian Radium Hospital, University of Oslo, Ullernchausseen 70-0310 Oslo, Norway

<sup>5</sup>Institute of Molecular Genetics, Czech Academy of Sciences, Flemingovo nam. 2, Praha 6, CZ-16637, Czech Republic

During the evolution of cancer, the incipient tumour experiences 'oncogenic stress', which evokes a counter-response to eliminate such hazardous cells. However, the nature of this stress remains elusive, as does the inducible anti-cancer barrier that elicits growth arrest or cell death. Here we show that in clinical specimens from different stages of human tumours of the urinary bladder, breast, lung and colon, the early precursor lesions (but not normal tissues) commonly express markers of an activated DNA damage response. These include phosphorylated kinases ATM and Chk2, and phosphorylated histone H2AX and p53. Similar checkpoint responses were induced in cultured cells upon expression of different oncogenes that deregulate DNA replication. Together with genetic analyses, including a genome-wide assessment of allelic imbalances, our data indicate that early in tumorigenesis (before genomic instability and malignant conversion), human cells activate an ATR/ATM-regulated DNA damage response network that delays or prevents cancer. Mutations compromising this checkpoint, including defects in the ATM–Chk2–p53 pathway, might allow cell proliferation, survival, increased genomic instability and tumour progression.

Tumorigenesis is an evolutionary process that selects for genetic and epigenetic changes, allowing evasion of anti-proliferative and cell-death-inducing mechanisms that normally limit clonal expansion of somatic cells<sup>1</sup>. Most tumours acquire genetic instability, but how early this occurs and whether it drives tumour development is unclear<sup>2</sup>. Several mechanisms to constrain oncogenesis have been proposed, including hypoxia<sup>3</sup>, telomere attrition<sup>4</sup> and induced expression of the Arf tumour suppressor (which is caused by the mitogenic overload experienced by incipient cancer cells)<sup>5</sup>. These are all conditions that can activate the tumour suppressor p53 (refs 1, 3–6). However, whether these mechanisms represent the major force(s) that guard against genetic instability and tumorigenesis is unknown. Recently, another possibility emerged from our observation<sup>7</sup> that advanced carcinomas of the lung and breast show constitutive activation of Chk2, an effector kinase<sup>8</sup> within the DNA damage network that is activated by the kinase ATM (Ataxia Telangiectasia Mutated) in response to DNA double-strand breaks<sup>9,10</sup>. Furthermore, oncogenes such as Myc cause DNA damage in cultured cells<sup>11,12</sup>. These findings led us to hypothesize that DNA damage checkpoints might become activated in the early stages of human tumorigenesis, leading to cell-cycle blockade or apoptosis and thereby constraining tumour progression.

## DNA damage signalling in early bladder tumours

To determine whether Chk2 is activated in premalignant human tumours, we compared early, superficial lesions (stage Ta), early invasive (T1) and more advanced stages (T2–4) of urinary bladder cancer, all untreated by radiation or chemotherapy. Contrary to the negative staining of normal tissues, immunohistochemistry using a well-characterized antibody<sup>7,8</sup> against activated Chk2 (phosphorylated at Thr 68) showed heterogeneous positive staining in the vast majority of the Ta lesions (Figs 1 and 2a). A similar pattern was seen in the T1 tumours, but the T2–4 carcinomas, although still commonly positive, showed moderately lower staining (Figs 1 and 2a).

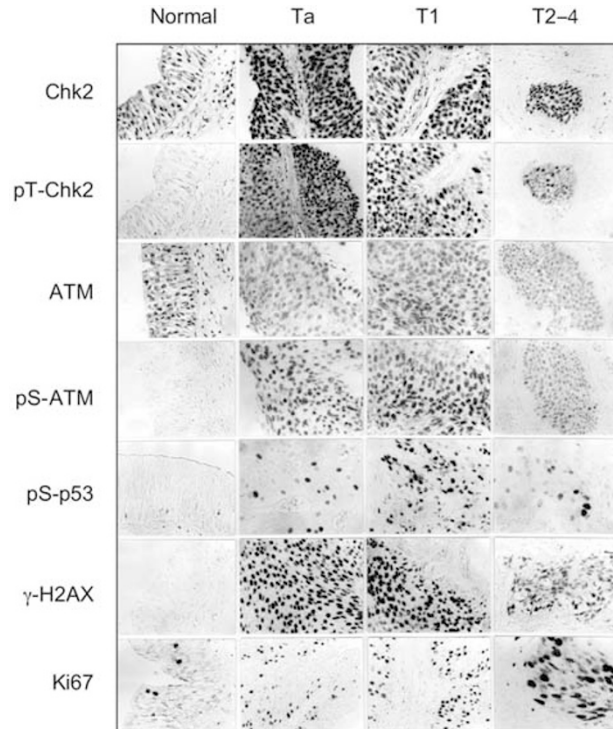


**Figure 1** Constitutive activation of the ATM–Chk2–p53 pathway in human urinary bladder cancer. Immunohistochemistry of normal uroepithelium, early superficial lesions (Ta), earliest invasive (T1) and more advanced primary carcinomas (T2–4). Chk2 and ATM proteins are ubiquitously expressed, but Thr 68-phosphorylated Chk2 (pT-Chk2), Ser 1981-phosphorylated ATM (pS-ATM), Ser 15-phosphorylated p53 (pS-p53) and Ser 139-phosphorylated histone H2AX (γ-H2AX) are detectable only in tumour tissues. They are all present at the early stages of tumour development. Ki67 is a marker of proliferating cells. Original magnification, ×100.

These results support our hypothesis and raise the possibility that the upstream kinase ATM, which normally phosphorylates Chk2 (on Thr 68) in response to double-strand break-causing insults such as ionizing radiation<sup>9,10</sup>, might be constitutively activated in tumours. Indeed, parallel tissue sections showed positive staining for Ser 1981-phosphorylated ATM, a marker of ATM auto-activation<sup>13</sup>, as well as for the ATM substrates p53 (phosphorylated on Ser 15) and histone H2AX (phosphorylated on Ser 139,  $\gamma$ -H2AX)<sup>10,13,14</sup> (Fig. 1 and Supplementary Figs S1, S2a).

### DNA damage response precedes p53 mutations

Another prediction arising from the idea that DNA damage checkpoints act as a barrier against cancer and genetic instability (and a pressure selecting for p53 mutations), is that ATM–Chk2 pathway activation must precede the occurrence of pronounced genomic instability and p53 aberrations. To address these issues, we examined DNA isolated from 35 microdissected bladder tumours (stages Ta, T1, T2–4) for allelic imbalances, comparing single-nucleotide polymorphisms (SNPs) in blood and tumour DNA from each patient. This genome-wide estimate of genomic (in)stability was obtained using SNP arrays<sup>15</sup>, which included some 10,000 probes, of which about 2,600 were averagely heterozygous (informative). Reflecting the frequency of expected heterozygosity (present in blood DNA) versus aberrantly reduced heterozygosity in the tumour, we subdivided the tumours into groups according to their proportion of allelic imbalances (low, intermediate and high genomic instability; see Methods and Supplementary Fig. S2c). Levels of Chk2 and ATM phosphorylation (detected by immunohistochemistry) were already maximal in the most stable subset of tumours, and therefore preceded the development of pronounced genomic instability (Fig. 2b and Supplementary Fig. S2b).

We then estimated the relationship between DNA damage response activation and potential defects in the ATM–Chk2–p53

pathway using loss of heterozygosity at the respective gene loci, immunohistochemical analysis of protein abundance (Chk2 and ATM), and direct DNA sequencing (*p53* and *CHK2*). These analyses revealed numerous abnormalities (Fig. 2c), including numerous *p53* mutations and a previously unidentified splice mutation of *CHK2* that was accompanied by loss of heterozygosity and lack of the Chk2 protein (Fig. 2d). Notably, whereas only one aberration was detected among the tumours classified as stable according to the SNP array data, eight defects were found in the intermediate subset and 24 aberrations were identified in the unstable lesions (Fig. 2c). These results show that the ATM–Chk2–p53 cascade<sup>7–10</sup> is activated in human bladder tumours before the occurrence of p53 mutations and/or defects in DNA damage signalling.

### Constitutive DNA damage is shared by early human lesions

Analogous to bladder carcinomas, Thr 68-phosphorylated Chk2 was detectable (at various levels) in the majority of 244 invasive carcinomas of the breast, colon or lung. This is in sharp contrast with negative samples from 87 normal, proliferating tissues (Fig. 3a, b and data not shown) and 26 inflammatory tissues (Supplementary Fig. S3). Furthermore, phosphorylated Chk2, ATM and H2AX were also found in the majority of pre-invasive carcinoma *in situ* (CIS, *n* = 55) lesions of the breast (Fig. 3a and data not shown), colorectal adenomas (Fig. 3b and see below) and lung hyperplasias (ref. 16 and data not shown). These data established that constitutive activation of the ATM–Chk2 pathway commonly occurs at pre-invasive stages of major types of human tumours.

### Oncogenes induce DNA damage response in cultured cells

The above results raise a question about the identity of tumorigenic events that could evoke the observed DNA damage response in human cancer. First, we tested for the effects of cyclin E over-expression (Fig. 4a), an event common in carcinomas and reported to enhance genomic instability<sup>17–21</sup>. In our U-2-OS-derived cells (a

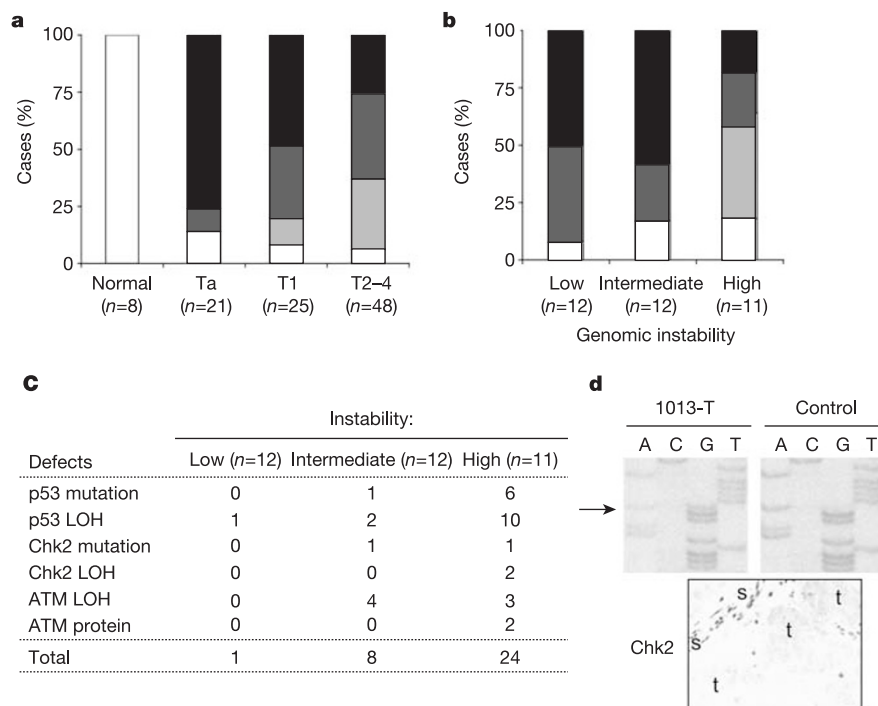


**Figure 2** Chk2 activation precedes p53 mutations and genomic instability in bladder cancer. **a, b**, Summary graphs of Thr 68-phosphorylated Chk2 (pT-Chk2) detected immunohistochemically in normal tissues and Ta, T1 and T2–4 lesions (**a**), and in lesions with different genomic instability (**b**). pT-Chk2 was either absent (white), or detected at low (light grey), medium (dark grey) or high (black) levels. **c**, Summary of tumour-

associated defects in the ATM–Chk2–p53 pathway in lesions with different genomic instability. LOH, loss of heterozygosity. **d**, Top panel, sequences of wild-type and mutant (1013-3T) *CHK2* DNA. The arrow highlights an A to G substitution in tumour DNA. Bottom panel, lack of Chk2 detection (by immunohistochemistry) in tumour (t) but not in stromal cells (s) of the corresponding tissue sample.

checkpoint-proficient human osteosarcoma cell line with wild-type retinoblastoma (RB) and p53), cyclin E could be overexpressed in a tetracycline-repressible manner to reach levels comparable with the endogenous protein in breast cancer cell lines containing increased copies of the cyclin E gene (Fig. 4b). Biochemical analysis of cells with induced cyclin E expression showed time-dependent increases in Ser 15-phosphorylated p53,  $\gamma$ -H2AX, and Ser 966-phosphorylated cohesin SMC1 (Fig. 4a); these are all targets of the DNA damage response kinases ATM and ATR<sup>9,10,14,22,23</sup>. Analogous to cyclin E, overexpression of tetracycline-regulatable Cdc25A<sup>24</sup>, another proto-oncogene overexpressed in many carcinomas<sup>24,25</sup>, evoked a DNA damage response (Fig. 4a). A similar response was also observed when oestrogen receptor-tagged E2F1 (ref. 26), an S-phase-promoting transcription factor commonly deregulated in cancer owing to aberrations of the RB pathway<sup>27</sup>, was translocated into the nucleus upon addition of tamoxifen to the medium (Fig. 4a).

Consistent with our biochemical data (Fig. 4), the checkpoint-mediated phosphorylation markers were also detectable cytologically (Fig. 5a, b and Supplementary Fig. S4a, b), and were reminiscent of the heterogeneous staining patterns seen in the clinical specimens (Figs 1 and 3). Although the oncogene-induced phosphorylation of Chk2 (on Thr 68) and ATM (on Ser 1981) were detectable both biochemically and cytologically, they were less pronounced than  $\gamma$ -H2AX. This suggests that the ATR–H2AX/Chk1 pathway<sup>9,10,23</sup> probably contributes to the overall response. Indeed, Chk1 was found to be phosphorylated on its activatory sites, Ser 317 and Ser 345 (Fig. 4c); of which Ser 345 is regarded as a preferential target for phosphorylation by ATR<sup>10,28,29</sup>. Phosphorylated Chk1 was also detected by fluorescence microscopy two days after induction of cyclin E, Cdc25A or E2F1 (Fig. 5a). Another established target of ATR phosphorylation, the checkpoint protein Rad17 (refs 10, 30), was also phosphorylated (on Ser 645; Fig. 4b). Analogous to U-2-OS cells, ectopic expression of cyclin E induced a DNA damage response in human fibroblasts (Supplementary Fig. S5).

Our cell culture models show that S-phase-promoting oncogenes can activate the ATM/ATR-regulated DNA damage network.

Furthermore, unlike phosphorylations of p53 and H2AX induced by the Myc oncogene, which are a consequence of oxygen radical generation<sup>11</sup>, the DNA damage response in our experiments was only marginally repressed by the antioxidant *N*-acetyl-L-cysteine (NAC; Fig. 4a and Supplementary Figs S4d, S5b, c). This indicates that the bulk of the DNA damage caused by the hyperproliferative oncogenic stimuli was independent of oxidative stress.

Because overexpressed cyclin E, Cdc25A and E2F1 share the ability to promote unscheduled S-phase entry<sup>26,31,32</sup>, we argue that the DNA damage response could reflect deregulated DNA replication rather than oxidative stress. When cells experience replicational stress, they activate their replication checkpoint to delay S phase progression and G2/M transition<sup>33</sup>. Consistent with this scenario, U-2-OS cells with induced cyclin E expression accumulated in S and G2 phases. The G2 arrest was particularly prominent by day 4 of time course experiments, and by day 6 many cells showed aberrantly enhanced DNA contents (>4n; Fig. 5c), probably reflecting partial re-replication of the genome uncoupled from cell division. The inability to enter mitosis correlated with massive induction of the Tyr 15-phosphorylated, inactive form of the key mitosis-promoting kinase Cdk1 (ref. 34; Fig. 5d), which is a marker of the effective checkpoint.

In further support of the idea that cyclin E overexpression alters replication dynamics, significantly longer replication tracks were detected using DNA fibre labelling<sup>35</sup>, and increased amounts of the single-stranded-(ss)DNA-binding replication protein A (RPA)<sup>36,37</sup> were bound to chromatin (Supplementary Fig. S4a, b). RPA loading on ssDNA occurs during normal replication initiation<sup>38</sup> and also on abnormal ssDNA intermediates that form during replicational stress<sup>36,39</sup>; the latter scenario is consistent with the hyperphosphorylation of RPA<sup>37</sup> in our experiments. Importantly, RPA-coated ssDNA is a prerequisite (and serves as an activation signal) for the ATR-dependent checkpoint<sup>36,39</sup>, and cyclin-induced aberrant DNA replication in yeast causes double-strand breaks<sup>40,41</sup>, potentially deadly lesions that activate the ATM–Chk2 pathway in mammals<sup>9,10,33</sup>.

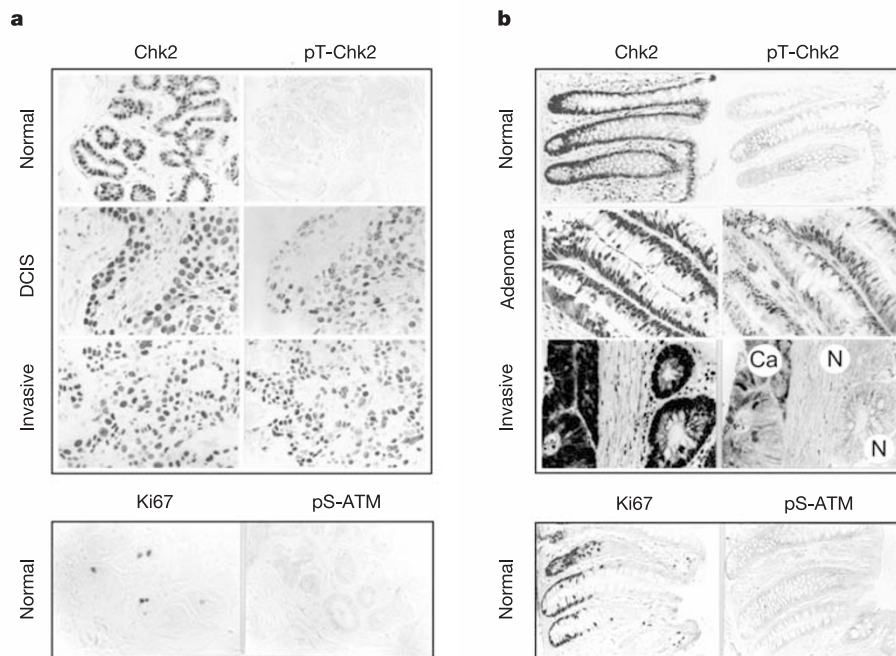


**Figure 3** Phosphorylation and activation of Chk2 in early breast and colon tumours. **a**, Immunohistochemical staining of total Chk2 and Thr 68-phosphorylated Chk2 (pT-Chk2) in normal breast, early lesion of ductal carcinoma *in situ* (DCIS), and invasive ductal carcinoma. Bottom panel, normal breast shows limited cell proliferation (Ki67 marker) and no Ser 1981-phosphorylated ATM (pS-ATM). **b**, Total Chk2 and pT-Chk2 in

normal colon, precursor lesion of exophytic adenoma, and invasive carcinoma. Note pT-Chk2 staining in the carcinoma (Ca) but not adjacent normal epithelium (N). Bottom: normal colon crypts show high cell proliferation (Ki67) but no pS-ATM. Original magnification,  $\times 100$  (**a**, **b**).

**Oncogenes and checkpoint activation in early tumours *in vivo***

Together, our cell culture experiments suggest that tumorigenic abnormalities that deregulate DNA replication induce DNA damage and checkpoint activation. To validate this concept for early tumorigenesis *in vivo*, three predictions should be verified: (1) tumorigenic abnormalities that deregulate entry into S phase must occur with high frequency; (2) there should be evidence for replicational stress; and (3) activation of a functional checkpoint should be documented. We were able to verify each of these three predictions for premalignant lesions, using the analyses described below.

First, we found cases with RB defects among the early bladder lesions, and the majority of Ta lesions showed overexpressed cyclin E and/or unscheduled cyclin E expression (Fig. 6a, c). In addition, 64% of these lesions showed activating mutations in fibroblast growth factor receptor 3 (FGFR3) (ref. 42, Fig. 6a); these abnormalities might induce the DNA damage response in a manner analogous to effects of growth factor overload in human epithelial xenografts<sup>16</sup>. Finally, over half of the colon adenoma samples showed unscheduled or overexpressed cyclin E (Fig. 6a–c), and this correlated well with the DNA damage response (monitored using  $\gamma$ -H2AX as a marker; Supplementary Fig. S6a, b). Cyclin E abundance and its unscheduled expression during the cell cycle, defined as a ratio of cyclin E-positive to Ki67-positive cells (Fig. 6b), provides a readout for defective RB–E2F and/or Myc pathways, for amplification of the cyclin E gene, and for mutations in the

human *CDC4* gene (the product of which controls cyclin E turnover)<sup>20,21,26,27,32</sup>. These results identify frequent aberrations of G1/S phase control in premalignant lesions.

Second, according to our proposal, double-strand breaks and loss of heterozygosity would probably occur at genomic sequences that are difficult to replicate: the fragile sites<sup>43</sup>. Consistent with this, our SNP array data showed that among the genetically most stable early lesions, loss of heterozygosity at known fragile sites occurs 3–15 times more often than expected from random targeting (Fig. 6e). This contrasts with only a twofold preference for loss of heterozygosity at fragile sites among the more advanced and genetically unstable bladder tumours. The exact degree of preference should be interpreted with caution, given that some fragile sites harbour tumour suppressor genes and that their loss might provide a growth advantage. However, we note that fragile sites are targeted during the period in which we observe maximal DNA damage response, and that ATR is involved in the maintenance of fragile sites<sup>43</sup>. Together with the emerging view that loss of heterozygosity at fragile sites is a ‘signature’ of stalled replication forks<sup>43</sup>, these observations support our proposed concept.

Third, to show unequivocally that the activated checkpoint machinery affects its downstream cell-cycle targets, we examined samples of normal colon and adenomas for Tyr 15-phosphorylated Cdk1 (pY-Cdk1). In normal colon, pY-Cdk1 staining was predominantly cytoplasmic, detectable within the proliferative compart-

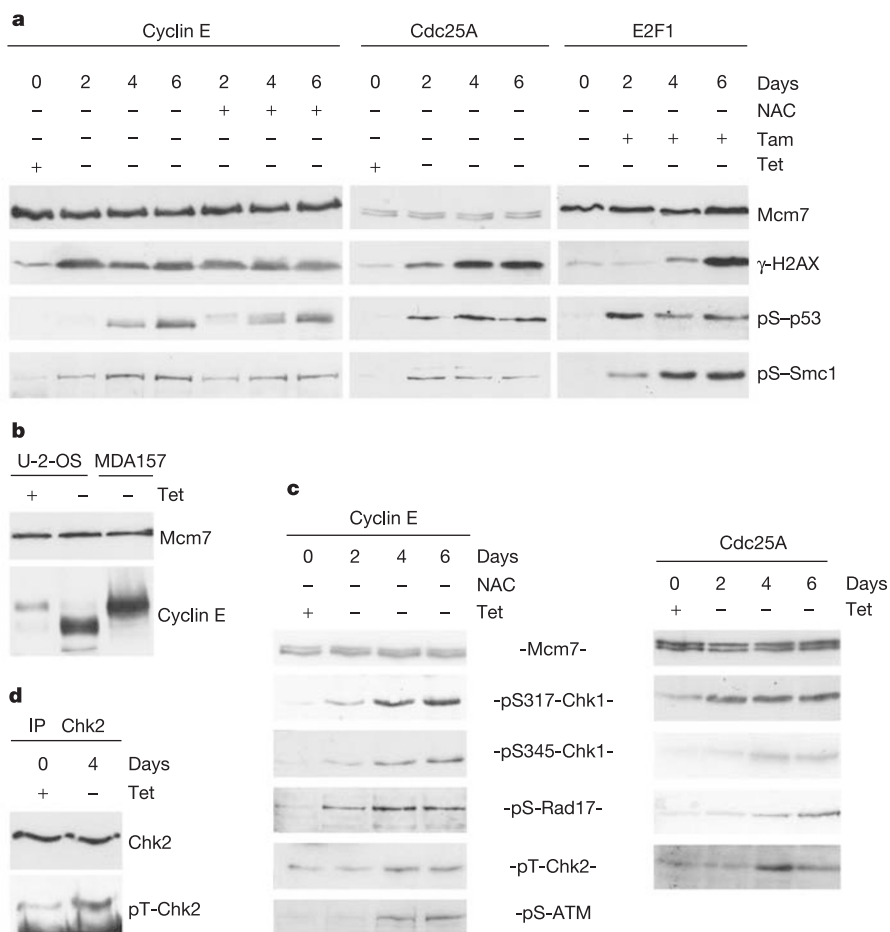


**Figure 4** Overexpressed cyclin E, Cdc25A and E2F1 induce a DNA damage response in U-2-OS cells. **a**, Time course immunoblotting analyses using the indicated phospho-specific antibodies. NAC, antioxidant *N*-acetyl-L-cysteine; Tam, tamoxifen; Tet, tetracycline; Mcm7, loading control. **b**, Immunoblots showing cyclin E abundance after a 2-day induction, compared with endogenous cyclin E levels in MDA157 cells with

amplified cyclin E gene. The altered mobility of ectopic cyclin E is explained in refs 31 and 32. **c**, Time course immunoblotting analyses using the indicated phospho-specific antibodies. **d**, Chk2 immunoprecipitates were analysed by immunoblotting for total Chk2 and pT-Chk2 before and 4 days after induction of cyclin E.

ment of the epithelial crypts in a modest fraction of cells (Fig. 6d). In contrast, over 50% of adenomas had enhanced pY-Cdk1, shown as higher staining intensity and larger groups or continuous sheets of positive cells (Fig. 6d). Staining of parallel sections revealed a good correlation between pY-Cdk1 and  $\gamma$ -H2AX (Fig. 6d and Supplementary Fig. S8a, c), consistent with the cell-cycle checkpoint being active in the same lesions (and the same areas within a lesion) that showed the DNA damage signalling. Reflecting their somewhat attenuated DNA damage response, invasive colorectal carcinomas showed less  $\gamma$ -H2AX and pY-Cdk1 staining than adenomas (Supplementary Fig. S8b). Finally, unlike in normal crypts where moderate pY-Cdk1 staining marked a subset of proliferating cells, the areas in adenomas strongly positive for pY-Cdk1 often showed only limited proliferation or were completely lacking in Ki67 staining (Supplementary Fig. S8c); this is consistent with prolonged cell-cycle arrest. These results indicate that the DNA damage response in precancerous lesions is functional and indeed affects the cell-cycle machinery.

Our data and those in ref. 16 suggest that tumorigenic events early in the progression of major human cancer types activate the ATR/ATM-regulated checkpoint through deregulated DNA replication and DNA damage, and thereby activate an inducible barrier against tumour progression and genetic instability (Fig. 6f). We

propose that candidate inducers of such a response include aberrations that grossly overstimulate growth factor pathways, affect RB or impair DNA replication downstream of RB (such as deregulated E2F1 (refs 25–27, 44) and overexpressed cyclin E<sup>17–21</sup> or Cdc25A<sup>24,25</sup>), and mutations in DNA repair genes such as *BRCA2* (ref. 45). The observed DNA damage might reflect abnormalities in pre-replication complex maturation and/or stalled or collapsed replication forks (which are known inducers of the ATR–H2AX/Chk1 cascade<sup>9,23,33,36,39</sup>), followed by the generation of double-strand breaks<sup>40,41,45</sup> and consequent activation of the ATM–H2AX/Chk2–p53 pathway<sup>8–10</sup>. We speculate that such responses might limit the progression of lesions, possibly contributing to long ‘latency’ periods or failure of early lesions to ever become malignant. Tumour progression under such circumstances probably relies on selection of cells defective in their DNA damage response components (such as ATM or p53), with compromised cell-cycle arrest, senescence and apoptosis. Oncogene-induced DNA damage, particularly double-strand breaks, might also enhance genomic instability, especially when checkpoint responses have been evaded.

Whether the DNA damage response reported here represents the predominant mode for constraining tumorigenesis remains to be established. However, it is apparent that p53 induction by the Arf tumour suppressor<sup>5</sup> cannot account for our data, because the DNA

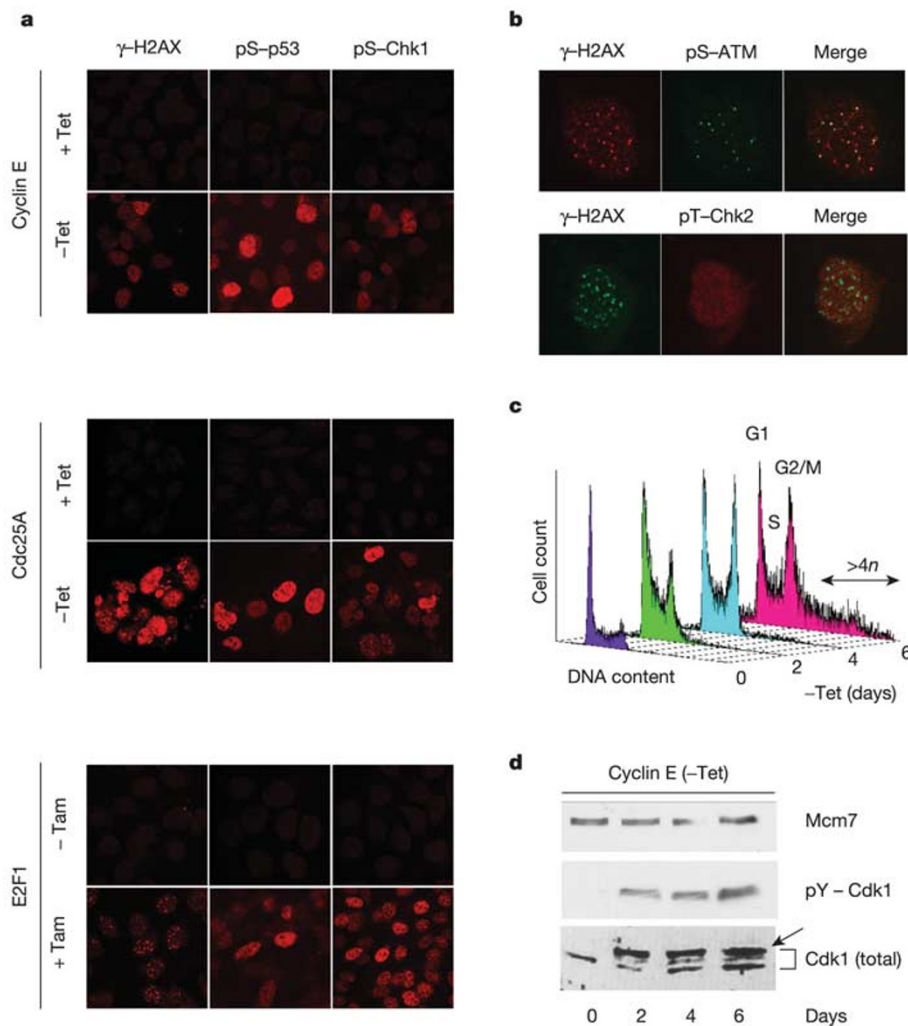


**Figure 5** DNA damage response to overexpressed oncogenes in U-2-OS cells. **a**, Confocal immunofluorescence microscopy images of cells stained for  $\gamma$ -H2AX, pS-p53 or pS-Chk1, after 4 days induction of cyclin E or Cdc25A (induced by removing tetracycline from the medium, –Tet), or induction of E2F1 (induced by tamoxifen (+Tam), causing translocation to the nucleus). **b**, Double-immunofluorescence colocalization of

$\gamma$ -H2AX and pS-ATM foci (top), and pT-Chk2 staining in  $\gamma$ -H2AX-foci-positive nuclei (bottom) in cells with induced cyclin E. **c**, Time course analysis of flow cytometry. **d**, Time course immunoblotting analysis of Mcm7 (loading marker), pY-Cdk1 and total Cdk1. Arrow shows the Tyr 15-phosphorylated form of Cdk1.

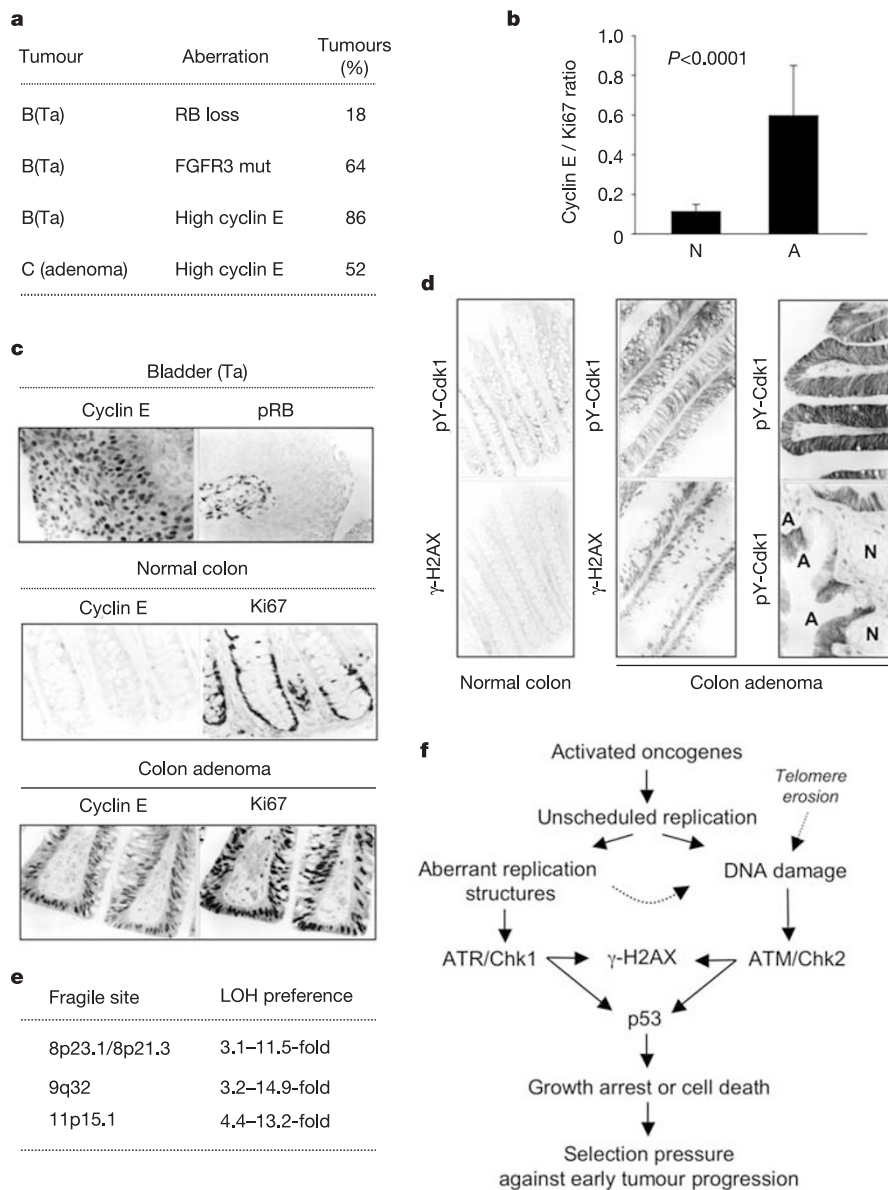


**Figure 6** Oncogenes and DNA damage response in early lesions. **a**, Tumorigenic aberrations in bladder (B) and colon (C) lesions. Frequent FGFR3 mutations ( $n = 33$ ) were R248C, S249C and Y375C. High cyclin E levels denote a cyclin E/Ki67-positive cell ratio over 0.5. **b**, Cyclin E/Ki67 ratios in normal colon (N;  $n = 30$ ) and adenomas (A;  $n = 29$ ). Data show means  $\pm$  s.d. **c**, Immunohistochemistry showing cyclin E overexpression and loss of RB protein (pRB) (top panel), and normal (middle panel) and high (bottom panel)

cyclin E/Ki67 ratios. **d**, Immunohistochemical staining of Tyr 15-phosphorylated Cdk1 (pY-Cdk1) and  $\gamma$ -H2AX in colon adenoma (A) and normal epithelium (N). **e**, Loss of heterozygosity (LOH) at fragile sites occurs preferentially (at higher than the expected (random) frequency) in the genetically most stable early bladder lesions. **f**, Model of the DNA damage response in tumorigenesis.

damage response does not rely on Arf<sup>1</sup>. On the other hand, telomere dysfunction, a phenomenon that might occur in premalignant tumours<sup>46,47</sup>, can mimic DNA damage and activate the ATM/ATR-dependent checkpoints, thereby contributing to replicative senescence in cultured cells<sup>48,49</sup>. We propose that oncogene-induced DNA damage and dysfunctional telomeres might converge to activate the DNA damage response, acting as a common mechanism to prevent progression of preneoplastic lesions (Fig. 6f). From a broader perspective, the DNA damage response machinery might play an important role in fundamental biological processes such as ageing and tumorigenesis. □

## Methods

### Antibodies

We used antibodies against total and Thr 68-phosphorylated Chk2 (refs 7 and 8), cyclin E (Novocastra Laboratories), cyclin A (Novocastra Laboratories),  $\gamma$ -H2AX (Upstate), RPA

p32 (Neomarkers), Ser 1981-phosphorylated ATM (Rockland or from C. Bakkenist and M. B. Kastan), ATM (from Y. Shiloh), Ki67 (Dako),  $\gamma$ -H2AX, Ser 15-phosphorylated p53, Ser 317-phosphorylated Chk1, Ser 345-phosphorylated Chk1 and Ser 645-phosphorylated Rad17 (all from Cell signalling), and Tyr 15-phosphorylated Cdk1 (Calbiochem) and Ser 966-phosphorylated Smc1 (Abcam).

### Immunohistochemistry

Tumours and control tissues were obtained from the tissue banks of four institutes in Denmark and Norway, with the approval of local ethical committees. The early lesions from bladder (Ta), breast (CIS) and lung (hyperplasias) showed broad spectra of histopathological grading, whereas the majority of colon adenomas were of high grade. Indirect immunoperoxidase staining on formaldehyde-fixed, de-paraffinized tissue sections or on formalin-fixed cultured cells was performed as described<sup>7</sup>, using the Vectastain Elite kit and nickel sulphate enhancement without nuclear counterstaining. The immunostaining patterns were evaluated by an experienced pathologist and scored as (1) negative (no positive staining or up to 1% of scattered positive cells); (2) low (heterogeneous staining, where an area corresponding to at least 20% of the section showed 2–10% positive cells); (3) medium (heterogeneous, with at least 20% of the section showing 10–50% positive cells); or (4) high positivity (variable to almost homogeneous

staining, with at least 20% of the section showing 51–90% positive cells).

**Cell culture**

Cells were grown in DMEM medium supplemented with 10% fetal calf serum and antibiotics. Construction, characterization and induction of U-2-OS-derived cell lines with tetracycline-repressible expression of human Cdc25A<sup>24</sup> and tamoxifen-inducible nuclear translocation and activity of human E2F1 (ref. 26) were performed as described. U-2-OS-derived cells with tetracycline-repressible expression of wild-type, full-length human cyclin E were constructed using previously reported methods and vectors<sup>24,32</sup>. Near-homogeneous expression of de-repressed cyclin E was seen in 90–95% of the cells by immunofluorescence, and despite the slightly altered gel mobility (owing to splicing also noticed in other regulatable systems<sup>31</sup>), the ectopic cyclin E was functional as judged from its selective binding to Cdk2 and stimulation of its kinase activity<sup>31,32</sup> (data not shown). Retrovirus-mediated expression of cyclin E in normal human diploid fibroblasts was achieved as described<sup>18</sup>.

**Biochemical analyses**

Procedures for gel electrophoresis, immunoblotting and immunoprecipitation followed published protocols<sup>8,32</sup>. For immunoprecipitation of total Chk2, we used 800 µg of cellular protein lysate and 10 µl of rabbit primary antibody (H-300:sc-9064, Santa Cruz).

**Immunofluorescence**

The fixation, permeabilization and immunofluorescence staining procedures, as well as the details of laser confocal microscopy, have been previously published<sup>8</sup>.

**Mutation analysis**

Genomic DNA from laser-microdissected tumour tissue or blood cells was examined for FGFR3 mutations by direct sequencing. Chk2 and p53 mutations were assessed using denaturing gradient gel electrophoresis of polymerase chain reaction (PCR)-amplified fragments that covered the entire coding sequence and all splice sites; any aberrantly migrating fragments were sequenced. The primers used for amplification will be provided upon request. The identified mutations in p53 included missense mutations and one mutation resulting in a stop codon downstream of the single-nucleotide deletion (C at position 482). Loss of heterozygosity was assessed using the SNP array data, on the basis of allelic imbalances detected by SNP probes within the regions of the Chk2, p53 and ATM genes. Both the SNPs and the genes were positioned according to the same build of the human genome sequence (the UCSC April 2003 assembly, version hg15, which is based on NCBI Build 33).

**SNP array analysis**

Tumours for DNA extraction were frozen immediately after surgery and stored at –80 °C. Before DNA extraction, the tumours were transferred to Tissue-Tek (Sakura Finetek) and tumour tissue was crudely microdissected from tumour sections (20-µm thick). Control DNA was purified from blood of the same patient. DNA was extracted from tumour tissue and blood using a PUREGENE protocol (Gentra SYSTEMS), according to the manufacturer's instructions. The DNA concentration was determined using a spectrophotometer, and diluted to a concentration of 50 ng µl<sup>-1</sup>. The Single Primer Assay Protocol for GeneChip Mapping 10K Early Access Array was performed according to the manufacturer's instructions (Affymetrix). We developed an algorithm based on a Hidden Markov Model to score allelic imbalances<sup>30</sup>. The numbers of SNPs heterozygous in blood DNA were compared with corresponding tumour DNA, and the tumours were divided into 3 groups as follows: high instability (from 1270–1720 heterozygous SNPs preserved in the tumour; n = 11); intermediate instability (1900–2360; n = 12) and low instability (2390–2603 heterozygous SNPs; n = 12). The frequency of loss of heterozygosity at fragile sites compared with other genomic sites was corrected for the number of SNPs in the fragile sites as a fraction of the total number of SNPs on the array.

Received 15 December 2004; accepted 18 February 2005; doi:10.1038/nature03482.

1. Lowe, S. W., Cepero, E. & Evan, G. I. Intrinsic tumour suppression. *Nature* **432**, 307–315 (2004).
2. Lengauer, C., Kinzler, K. W. & Vogelstein, B. Genetic instabilities in human cancers. *Nature* **396**, 643–649 (1998).
3. Graeber, T. G. *et al.* Hypoxia induces accumulation of p53 protein, but activation of a G1-phase checkpoint by low-oxygen conditions is independent of p53 status. *Mol. Cell. Biol.* **14**, 6264–6277 (1994).
4. Counter, C. M. *et al.* Telomere shortening associated with chromosome instability is arrested in immortal cells which express telomerase activity. *EMBO J.* **11**, 1921–1929 (1992).
5. Zindy, F. *et al.* Arf tumour suppressor promoter monitors latent oncogenic signals in vivo. *Proc. Natl Acad. Sci. USA* **100**, 15930–15935 (2003).
6. Vogelstein, B., Lane, D. & Levine, A. J. Surfing the p53 network. *Nature* **408**, 307–310 (2000).
7. DiTullio, R. A. Jr *et al.* 53BP1 functions in an ATM-dependent checkpoint pathway that is constitutively activated in human cancer. *Nature Cell Biol.* **4**, 998–1002 (2002).
8. Lukas, C., Falck, J., Bartkova, J., Bartek, J. & Lukas, J. Distinct spatiotemporal dynamics of mammalian checkpoint regulators induced by DNA damage. *Nature Cell Biol.* **5**, 255–260 (2003).
9. Kastan, M. B. & Bartek, J. Cell-cycle checkpoints and cancer. *Nature* **432**, 316–323 (2004).
10. Shiloh, Y. ATM and related protein kinases: safeguarding genome integrity. *Nature Rev. Cancer* **3**, 155–168 (2003).
11. Vafa, O. *et al.* c-Myc can induce DNA damage, increase reactive oxygen species, and mitigate p53 function: a mechanism for oncogene-induced genetic instability. *Mol. Cell* **9**, 1031–1044 (2002).
12. Lindström, M. S. & Wiman, K. G. Myc and E2F1 induce p53 through p14ARF-independent mechanisms in human fibroblasts. *Oncogene* **22**, 4993–5005 (2003).
13. Bakkenist, C. J. & Kastan, M. B. DNA damage activates ATM through intermolecular autophosphorylation and dimer dissociation. *Nature* **421**, 499–506 (2003).
14. Rogakou, E. P., Pilch, D. R., Orr, A. H., Ivanova, V. S. & Bonner, W. M. DNA double-stranded breaks

- induce histone H2AX phosphorylation on serine 139. *J. Biol. Chem.* **273**, 5858–5868 (1998).
15. Lindblad-Toh, K. *et al.* Loss-of-heterozygosity analysis of small-cell lung carcinomas using single-nucleotide polymorphism arrays. *Nature Biotechnol.* **18**, 1001–1005 (2000).
16. Gorgoulis, V. G. *et al.* Activation of the DNA damage checkpoint and genomic instability in human precancerous lesions. *Nature* doi:10.1038/nature03485 (this issue).
17. Spruck, C. H., Won, K. A. & Reed, S. I. Deregulated cyclin E induces chromosome instability. *Nature* **401**, 297–300 (1999).
18. Minella, A. C. *et al.* p53 and p21 form an inducible barrier that protects cells against cyclin E-cdk2 deregulation. *Curr. Biol.* **12**, 1817–1827 (2002).
19. Ekholm-Reed, S. *et al.* Deregulation of cyclin E in human cells interferes with prereplication complex assembly. *J. Cell Biol.* **165**, 789–800 (2004).
20. Reed, S. E. *et al.* Mutation of hCDC4 leads to cell cycle deregulation of cyclin E in cancer. *Cancer Res.* **64**, 795–800 (2004).
21. Rajagopalan, H. *et al.* Inactivation of hCDC4 can cause chromosomal instability. *Nature* **428**, 77–81 (2004).
22. Kim, S. T., Xu, B. & Kastan, M. B. Involvement of the cohesin protein, Smc1, in Atm-dependent and independent responses to DNA damage. *Genes Dev.* **16**, 560–570 (2002).
23. Ward, I. M. & Chen, J. Histone H2AX is phosphorylated in an ATR-dependent manner in response to replicational stress. *J. Biol. Chem.* **276**, 47759–47762 (2001).
24. Mailand, N. *et al.* Rapid destruction of human Cdc25A in response to DNA damage. *Science* **288**, 1425–1429 (2000).
25. Cangi, M. G. *et al.* Role of the Cdc25A phosphatase in human breast cancer. *J. Clin. Invest.* **106**, 753–761 (2000).
26. Müller, H. *et al.* E2Fs regulate the expression of genes involved in differentiation, development, proliferation, and apoptosis. *Genes Dev.* **15**, 267–285 (2001).
27. Bartek, J., Bartkova, J. & Lukas, J. The retinoblastoma protein pathway in cell cycle control and cancer. *Exp. Cell Res.* **237**, 1–6 (1997).
28. Zhao, H. & Piwnicka-Worms, H. ATR-mediated checkpoint pathways regulate phosphorylation and activation of human Chk1. *Mol. Cell. Biol.* **21**, 4129–4139 (2001).
29. Gatei, M. *et al.* ATM and NBS1-dependent phosphorylation of Chk1 on Ser-317 in response to ionizing radiation. *J. Biol. Chem.* **278**, 14806–14811 (2003).
30. Bao, S. *et al.* ATR/ATM-mediated phosphorylation of human Rad17 is required for genotoxic stress responses. *Nature* **411**, 969–974 (2001).
31. Resnitzky, D., Gossen, M., Bujard, H. & Reed, S. I. Acceleration of the G1/S phase transition by expression of cyclins D1 and E with an inducible system. *Mol. Cell. Biol.* **14**, 1669–1679 (1994).
32. Santoni-Rugiu, E., Falck, J., Mailand, N., Bartek, J. & Lukas, J. Involvement of Myc activity in a G1/S-promoting mechanism parallel to the pRB/E2F pathway. *Mol. Cell. Biol.* **20**, 3497–3509 (2000).
33. Bartek, J., Lukas, C. & Lukas, J. Checking on DNA damage in S phase. *Nature Rev. Mol. Cell Biol.* **5**, 792–804 (2004).
34. Lew, D. J. & Kornbluth, S. Regulatory roles of cyclin dependent kinase phosphorylation in cell cycle control. *Curr. Opin. Cell Biol.* **8**, 795–804 (1996).
35. Merrick, C. J., Jackson, D. & Diffley, J. F. X. Visualization of altered replication dynamics after DNA damage in human cells. *J. Biol. Chem.* **279**, 20067–20075 (2004).
36. Zou, L. & Elledge, S. J. Sensing DNA damage through ATRIP recognition of RPA-ssDNA complexes. *Science* **300**, 1542–1548 (2003).
37. Binz, S. K., Sheehan, A. M. & Wold, M. S. Replication protein A phosphorylation and the cellular response to DNA damage. *DNA Repair (Amst.)* **3**, 1015–1024 (2004).
38. Walter, J. & Newport, J. Initiation of eukaryotic DNA replication: origin unwinding and sequential chromatin association of Cdc45, RPA and DNA polymerase  $\alpha$ . *Mol. Cell* **5**, 617–627 (2000).
39. Osborn, A. J., Elledge, S. J. & Zou, L. Checking on the fork: the DNA-replication stress-response pathway. *Trends Cell Biol.* **12**, 509–516 (2002).
40. Tanaka, S. & Diffley, J. F. Deregulated G1-cyclin expression induces genomic instability by preventing efficient pre-RC formation. *Genes Dev.* **16**, 2639–2649 (2002).
41. Lengronne, A. & Schwob, E. The yeast CDK inhibitor Sic1 prevents genomic instability by promoting replication origin licensing in late G1. *Mol. Cell* **9**, 1067–1078 (2002).
42. Hart, K. C. *et al.* Transcription and Stat activation by derivatives of FGFR1, FGFR3, and FGFR4. *Oncogene* **19**, 3309–3320 (2000).
43. Casper, A. M., Nghiem, P., Arlt, M. F. & Glover, T. W. ATR regulates fragile site stability. *Cell* **111**, 779–789 (2002).
44. Rogoff, H. A. *et al.* Apoptosis associated with deregulated E2F activity is dependent on E2F1 and Atm1/Nbs1/Chk2. *Mol. Cell. Biol.* **24**, 2968–2977 (2004).
45. Lomonosov, M., Anand, S., Sangrithi, M., Davies, R. & Venkitaraman, A. R. Stabilization of stalled DNA replication forks by the BRCA2 breast cancer susceptibility protein. *Genes Dev.* **17**, 3017–3022 (2003).
46. Meeker, A. K. *et al.* Telomere length abnormalities occur early in the initiation of epithelial carcinogenesis. *Clin. Cancer Res.* **10**, 3317–3326 (2004).
47. Chin, K. *et al.* In situ analyses of genome instability in breast cancer. *Nature Genet.* **36**, 984–988 (2004).
48. d'Adda di Fagagna, F. *et al.* DNA damage checkpoint response in telomere-initiated senescence. *Nature* **426**, 194–198 (2003).
49. Takai, H., Smogorzewska, A. & de Lange, T. DNA damage foci at dysfunctional telomeres. *Curr. Biol.* **13**, 1549–1556 (2003).
50. Eddy, S. R. Profile hidden Markov models. *Bioinformatics* **14**, 755–763 (1998).

**Supplementary Information** accompanies the paper on [www.nature.com/nature](http://www.nature.com/nature).

**Acknowledgements** We thank Y. Shiloh, C. Bakkenist, M. Kastan, M. Welcker, B. Clurman, V. Gorgoulis and K. Helin for reagents; M.H. Lee, D. Lützhof, A. Arnt Kjerulf and L.-L. Christensen for technical assistance; and C. Wiuf for data analysis. This work was supported by the Danish Cancer Society, the Alfred Benzon Foundation and the European Commission.

**Competing interests statement** The authors declare that they have no competing financial interests.

**Correspondence** and requests for materials should be addressed to J.B. ([jb@cancl.dk](mailto:jb@cancl.dk)).